Exciton Hierarchies in Gapped Carbon Nanotubes

Robert M. Konik

Phys. Rev. Lett. **106**, 136805 — Published 29 March 2011

DOI: 10.1103/PhysRevLett.106.136805

Exciton Hierarchies in Gapped Carbon Nanotubes

Robert M. Konik[1]

[1] *Condensed Matter Physics and Material Science Department, Brookhaven National Laboratory, Upton, NY 11973*

We present evidence that the strong electron-electron (e-e) interactions in gapped carbon nanotubes lead to finite hierarchies of excitons within a given nanotube subband. We study these hierarchies by employing a field theoretic reduction of the gapped carbon nanotube permitting e-e interactions to be treated exactly. We analyze this reduction by employing a Wilsonian-like numerical renormalization group. We are so able to determine the gap ratios of the one-photon excitons as a function of the effective strength of interactions. We also determine within the same subband the gaps of the two-photon excitons, the single particle gaps, as well as a subset of the dark excitons. The strong e-e interactions in addition lead to strongly renormalized dispersion relations where the consequences of spin-charge separation can be readily observed.

PACS numbers: 72.15Qm,73.63Kv,73.23Hk

Gapped carbon nanotubes are the subject of intense experimental [1–6] and theoretical interest [7–17] due to their possible application as opto-electronic devices [1] as well as providing a particularly clean realization of strongly correlated electron physics in low dimensions [9, 17]. Both interests converge in the study of the tubes' excitonic spectra. This spectra, due to the effects of a strong Coulomb interaction in one dimension, is strongly renormalized from what would be expected from the underlying band structure of the tube. Its computation therefore requires a non-perturbative approach.

The favoured theoretical approach to studying the excitonic spectra of carbon nanotubes is the use of a Bethe-Salpeter equation combined with first principle input to approximate the particle and hole wavefunctions that form the excitons [10, 11, 13, 15]. This approach has been particularly valuable in that it has allowed a quantitative description of aspects of excitonic physics, in particular the magnitude of the excitonic gap for the lowest lying excitons in a given subband of the nanotube. In this letter we step away from trying to describe quantitative details of the excitons and instead focus on more qualitative features. We do so using an approach that combines a field theoretic reduction of the nanotubes identical to that used to study Luttinger liquid behaviour in metallic nanotubes with a numerical renormalization group that enables one to study the effects of gapping out a multi-component Luttinger liquid. In the process we find in a regime of strong e-e interactions a number of new features to the excitonic spectra (see Fig. 1).

First and foremost we find that a given subband of the nanotube has a finite number of optically active one-photon excitons, $\Delta^{1u,i}$, where the multiplicity depends on the strength of the tube's screened Coulomb interaction. While a simple picture of excitons as analogs of the excited states of a hydrogen atom [7] yields an infinite hierarchy of excitons, we argue this series is truncated to at most three. In order to understand the excitons' binding energy, we also study the single particle spectrum of the tube. The single particle gap is strongly renormalized by interactions and can be many multiples of the bare bandgap. Consequently the lowest lying two-excitation continuum, depending on strength of the Coulomb interaction, may be a particle-hole continuum *or* it may be a two-exciton continuum. This approach treats all excitations of the nanotube on the same footing. It thus conflates the difference between an exciton and a bi-exciton. Indeed interactions can be sufficiently strong that excitons should then be thought of equally as particle-hole bound states or bound states of two other excitons.

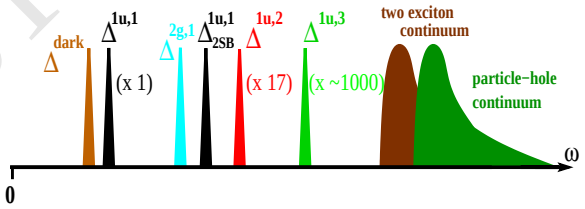

FIG. 1: A schematic indicating the position in energy of the various excitons together with two-excitation continua arising from our treatment at larger values of the effective interaction ($K_{c+}^{-1} \geq 5$). The bracketed numbers are estimates computed at $K_{c+} = 1/7$ of the absorption strength of the optically active excitons, $\Delta^{1u,1-3}$ relative to $\Delta^{1u,1}$.

Our results are applicable both to semiconducting nanotubes and metallic nanotubes which have been turned semiconducting by the application of an axial magnetic field [8]. We derive results in the infinite bandwidth limit. In the latter case where the gap is tunable and can be made much smaller than the bandwidth this limit is directly accessible. However we find that our results remain quantitatively accurate for gaps, Δ, an appreciable fraction of the bandwidth, D, and even qualitatively accurate for $\Delta \sim D$.

We focus on a single subband of a carbon nanotube. To describe this subband at low energies we introduce four sets (two for the spin, σ, degeneracy and two for the valley, $\alpha = K, K'$, degeneracy) of right ($r = +$)

and left ($r = -$) moving fermions, $\psi_{r\alpha\sigma}$. The Hamiltonian governing these fermions can be written as $H = \int dx(H_{kin}+H_{gap})+H_{Coulomb}$. $H_{kin}+H_{gap}$ together give the non-interacting band dispersion, $\epsilon^2(p) = v_0^2p^2 + \Delta_0^2$:

$$H_{kin} = -iv_0\psi^\dagger_{r\alpha\sigma}\partial_x\psi_{r\alpha\sigma}; \quad H_{gap} = \Delta_0\psi^\dagger_{r\alpha\sigma}\psi_{-r\alpha\sigma}, \quad (1)$$

where v_0 is the bare velocity of the fermions and repeated indices are summed. For the Coulombic part of the Hamiltonian we include only the strongest part of forward scattering:

$$H_{Coulomb} = \frac{1}{2}\int dxdx'\rho(x)V_0(x-x')\rho(x'),$$

where $\rho(x) = \sum_{r\alpha\sigma}\psi^\dagger_{r\alpha\sigma}(x)\psi_{r\alpha\sigma}(x)$. The remaining forward scattering terms as well as backscattering and Umklaap terms arising from the Coulomb interactions only lead to weak deviations (on the order of a few percent) to the gaps –unsurprising as they are less relevant, in the RG sense, than the gap term. But as they lift the model's SU(4) symmetry, they will split the lowest lying 15-fold multiplet of optically dark excitons.

To study the full Hamiltonian, we treat H_{gap} as a perturbing term (albeit one to be treated non-perturbatively) of $H_0 \equiv \int dx(H_{kin}) + H_{Coulomb}$. The latter terms are nothing more than the Hamiltonian of a metallic carbon nanotube. In excitonic language, we thus think of H_{gap} as a confining interaction on top of the metallic tube. The advantage of doing so is that we are able to treat Coulomb interactions *analytically exactly* at the beginning of the computation. We do so using bosonization.

If we bosonize H_0 in terms of chiral bosons $\phi_{r\alpha\sigma}$ by writing $\psi_{r\alpha\sigma} \sim \exp(i\phi_{r\alpha\sigma})$, we arrive at a simple result [17, 18]. The theory is equivalent to four Luttinger liquids described by the four bosons θ_i, $i = c_\pm, s_\pm$ (and their duals ϕ_i)

$$H_0 = \int dx \sum_i \frac{v_i}{2}\Big(K_i(\partial_x\phi_i)^2 + K_i^{-1}(\partial_x\theta_i)^2\Big). \quad (2)$$

The four bosons diagonalizing H_0 are linear combinations of the original four bosons and represent an effective charge-flavour separation where $\theta_{c+} = \sum_{r\alpha\sigma} r\tilde{\psi}_{r\alpha\sigma}$ is the charge boson and the remaining three bosons reflect the spin, valley, and parity symmetries in the problem. The charge boson is the only boson to see the effects of the Coulomb interaction. Both the charge Luttinger parameter K_{c+} and the charge velocity $v_{c+} = v_0/K_{c+}$ are strongly renormalized. In particular for long range Coulomb interactions, K_{c+} takes the form

$$K_{c+} = \left(1 + \frac{8e^2}{\pi\kappa\hbar v_0}\big(\log(\frac{L}{2\pi R}) + c_0\big)\right)^{-1/2}, \quad (3)$$

where κ is the dielectric constant of the substrate, L is the length of the nanotube, R is the tube's radius, and c_0 is a wrapping vector dependent $O(1)$ constant[16]. In typical nanotubes K_{c+} can take on values in the range of $\sim .2$. With an electric field applied transversely to the tube, K_{c+} can easily be made as small as .1 [16]. The remaining Luttinger parameters, K_i, $i = c_-, s_\pm$ retain their non-interacting values, 1, and so their velocities, $v_i = v_0$ go unrenormalized. Including the full forward scattering leads to a small (upwards) renormalization (on the order of less than a percent) of these parameters which we will not consider here [17].

Under bosonization, H_{gap} becomes

$$H_{gap} = \frac{4\tilde{\Delta}_0}{\pi}(\prod_i \cos(\frac{\theta_i}{2}) + \prod_i \sin(\frac{\theta_i}{2})), \quad (4)$$

where $\tilde{\Delta}_0 = \Delta_0(\Lambda/v_{c+})^{(1-K_{c+})/4}$ and Λ is an effective bandwidth of the tube arising from bosonization (and not equal to the tube's true bandwidth). This gap term is highly relevant. Rewriting the gap term in this fashion already gives us important generic features of the excitonic spectrum. Firstly, as a perturbation of H_0, H_{gap} has the anomalous dimension, $3/4 + K_{c+}/4$. In turn this implies the full gaps, $\{\Delta_\alpha\}_\alpha$, satisfy the scaling relation,

$$\Delta_\alpha = \Lambda(\frac{\Delta_0}{\Lambda})^{4/(5-K_{c_+})} f_\alpha(K_{c+}), \quad (5)$$

where $\{f_\alpha\}_\alpha$ is a set of *a priori* unknown dimensionless functions of K_{c+}. We will see that for the excitons, f_{Exc} is a relatively weak function of K_{c+} while for the single particle excitations, f_{sp} depends strongly on K_{c+}. This scaling relation tells us immediately how exciton gaps scale between subbands. If we take a large radius tube where the first and second subband gaps scale as $\Delta_0(n, R) \sim n/R$, $n = 1, 2$, the expected gap ratio between the two is $2^{4/(5-K_{c+})} \sim 1.78$ (this is in rough correspondence to that reported in [2] and so provides a straightforward explanation of the ratio problem [12]). Secondly, H_{gap} takes the form of a perturbation of a generalized sine-Gordon model (involving four bosons instead of one). We thus expect that excitons (within a given subband) will come in hierarchies whose size is determined by the value of K_{c+} very much like the number of bound states in a sine-Gordon model, a perturbation on a free boson of the form $\cos(\beta\theta)$, is determined by the parameter β.

Having completely characterized H_0, we study the confining effects of H_{gap} using the truncated conformal spectrum approach (TCSA) [19] combined with a Wilsonian renormalization group modeled after the numerical renormalization group (NRG) used to study quantum impurity problems [20]. This methodology permits the study of arbitrary continuum one dimensional theories provided one can write the theory as the sum of a gapless theory, in this case H_0, plus a perturbation, here H_{gap}. It is flexible enough that it can play the same role as DMRG does for lattice models (although as it is an

NRG, it accesses matrix elements more easily). Among the first uses of the original TCSA, unequipped with an NRG, was to study a quantum Ising model in a magnetic field [19]. The model we study here, in terms of computational complexity, is equivalent to eight coupled Ising models and so could not be studied using the TCSA without the accompanying NRG. Additional details of the application of this approach can be found in Ref. [21].

Our results for the gaps as a function of K_{c+} are presented in Fig. 2 (with details of of the numerical analysis relegated to Ref. [21]). We first consider the one-photon optically active excitons (labelled $\Delta^{1u,i}$, $i = 1, 2, 3$ where here u refers to the antisymmetry under $\pi-$rotations about the centre of a carbon hexagon). We see that as K_{c+} decreases (i.e. the effective Coulomb interactions become stronger) the number of one photon excitons grows. At $K_{c+} \geq 1/5$ the number of such excitons goes from one to two, while at $K_{c+} \geq 1/6$ the number of such excitons goes from two to three. But thereafter this number saturates. Our finding of three stable excitons for $K_{c+} \leq 1/6$ is robust: it survives even when $\Delta^{1u,3} \sim D/2$ where D is the bandwidth.

There are two limits on stable excitons in the system – the beginnings of both the particle-hole continuum (marked in dark green in Fig. 2) and a two-exciton continuum (marked in maroon in Fig. 2). Necessarily exciton gaps cannot cross over these boundaries lest a decay channel opens to the exciton. The bottom of the particle-hole continuum is twice the single particle gap, $2\Delta^{sp}$. As Δ^{sp} is a strong function of K_{c+} (going as $\Delta^{sp} \sim K_{c+}^{-1}$), at small K_{c+} there is room for additional excitons. This is very much like the sine-Gordon model where as β goes to zero, the number of bound states goes to infinity. However for an exciton to be stable it must also fall below a two-exciton continuum. This two-exciton continuum, formed from the lowest single-photon exciton, $\Delta^{1u,1}$, and the lowest two-photon exciton, $\Delta^{2g,1}$, is relatively insensitive to K_{c+} and serves to provide a bound on the total number of possible excitons at small K_{c+}.

In bosonized models considerable intuition can be had by considering the classical limit and asking what are the classical field solutions that correspond to the excitons/bound states. This is true here as well. The first one-photon exciton, $\Delta^{1u,i}$, corresponds to a breather-like solution of the field equations governing $H_0 + H_{gap}$. This solution corresponds to θ_{c+} interpolating between 0 to 4π and back to 0 while the other three bosons remain fixed at 0. It takes the form

$$\theta_{c+}(x,t) = 4\tan^{-1}\frac{\sqrt{1-\omega^2}\cos(\omega t)}{\omega\cosh(\sqrt{1-\omega^2}x)}, \qquad (6)$$

where ω is related to the (classical) energy of the breather. We can estimate the energy corresponding to quantizing this classical solution via mean field theory. Replacing H_{gap} by $4\tilde{\Delta}_0/\pi\Xi^3\cos(\theta_{c+}/2)$, where $\Xi \equiv \langle\cos(\theta_f/2)\rangle$ with $\theta_f = \theta_{c-}, \theta_{s+}$, or θ_{s-}, we reduce the model to a pure sine-Gordon theory. $\Delta^{1u,1}$ is then equal to the gap of this theory's first bound state [23]

$$\Delta^{1u,1}_{MFT} = 2\big(2\tilde{\Delta}_0\Xi^3\frac{\Gamma(1-\frac{\alpha}{2})}{v_{c+}^{\alpha-1}\Gamma(\frac{\alpha}{2})}\big)^{\frac{1}{2-\alpha}}\frac{2\Gamma(\frac{\xi}{2})\sin(\frac{\pi\xi}{2})}{\sqrt{\pi}\Gamma(\frac{1}{2}+\xi)}, \qquad (7)$$

where $\alpha = 1/4K_{c+}^2$ and $\xi = \alpha/(2-\alpha)$. Ξ is determined self-consistently by replacing H_{gap} with $4\tilde{\Delta}_0\pi^{-1}\Xi^2\langle\cos(\theta_{c+}/2)\rangle\cos(\theta_f/2)$ and using [22] to express Ξ in terms of the effective coupling constant $4\tilde{\Delta}_0\pi^{-1}\Xi^2\langle\cos(\theta_{c+}/2)\rangle$. We consequently find that as K_{c+}^{-1} varies between 2 and 10, $\Delta^{1u,1}_{MFT}/(\Lambda(\Delta_0/\Lambda)^{4/(5-K_{c+})})$ varies from 3.1 to 4.1 in reasonable agreement (if shifted upwards) with the non-perturbative NRG.

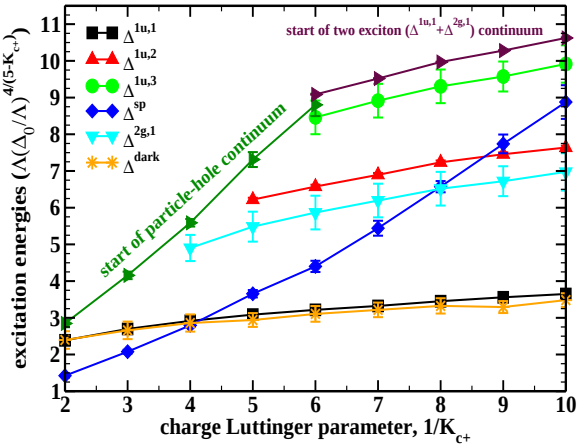

FIG. 2: The K_{c+} behavior of the excitons and single particles.

The second one-photon exciton, $\Delta^{1u,2}$, has a gap a little more than twice that of $\Delta^{1u,1}$ and corresponds to roughly the putative location of $\Delta^{1u,1}_{2\ SB}$, the first exciton in the second subband (which we have argued, by scaling, is found at $\sim 1.8\Delta^{1u,1}$). If we were to take into account intersubband Coulomb interactions, hitherto ignored, $\Delta^{1u,2}$ and $\Delta^{1u,1}_{2\ SB}$ would mix leading to a set of hybridized states. It is thus conceivable that reports of observations of the exciton $\Delta^{1u,1}_{2\ SB}$ are in fact seeing $\Delta^{1u,2}$ or at least some hybridized combination of the two.

Beyond the one-photon excitons, Fig. 2 also displays the gaps of a number of other excitons. It shows the single existing two-photon exciton, $\Delta^{2g,1}$ (here g corresponds to excitons which are symmetrical under π-rotations about a centre of a carbon hexagon). Unlike the one-photon excitons, there is only a single stable two-photon exciton regardless of the value of K_{c+}. Lying just below $\Delta^{1u,1}$ are found a set of 15 dark excitons with energy Δ^{dark}. These excitons subsume the dark triplet excitons but are of greater degeneracy because they not only carry spin quantum numbers but valley quantum numbers as well (dark excitons with non-trivial valley quantum number were termed K-momentum excitons in

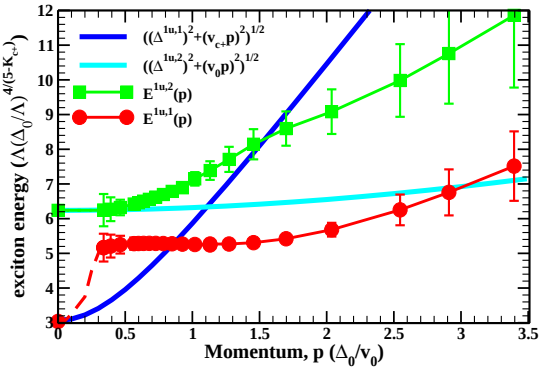

FIG. 3: The dispersion of the first two excitons $\Delta^{1u,1}$ and $\Delta^{1u,2}$ for $K_{c+} = 1/5$. Dashed lines in the small momentum regions connecting data points are guides to the eye.

Ref. [5]). As the full symmetry of H is SU(4), the dark excitons transform as SU(4)'s adjoint. At twice the energy of Δ^{dark} begins a two exciton continuum into which any two-photon exciton will decay. As $\Delta^{2g,1}$ is just below $2\Delta^{dark}$, this two exciton continuum essentially precludes any two-photon excitons with energy greater than $\Delta^{2g,1}$.

By examining the momentum dependence of the excitons' dispersions, we can see the consequences of having two velocities, charge, v_{c+}, and flavour $v_0 = v_{c-}, v_{s\pm}$, in the system. The above semiclassics suggests that the initial dispersion of $\Delta^{1u,1}$, $E^{1u,1}(p)$, will behave approximately as $((\Delta^{1u,1})^2 + p^2 v_{c+}^2)^{1/2}$ (a consequence of it involving θ_{c+} degrees of freedom alone). We expect $\Delta^{1u,2}$, to lie primarily in the spin/flavor sector and so it will disperse with the much smaller velocity, v_0. While $\Delta^{1u,2} > \Delta^{1u,1}$, that $v_{c+} \gg v_0$ means the dispersion of $\Delta^{1u,1}$ will intersect $\Delta^{1u,2}$ at a (small) momentum, $p_{int} = (((\Delta^{1u,2})^2 - (\Delta^{1u,1})^2)/(v_{c+}^2 - v_0^2))^{1/2}$. At this intersection the two states will hybridize, and so for momenta larger than p_{int}, $\Delta^{1u,1}(p > p_{int})$ will disperse with an effective mass determined by v_0 whereas $\Delta^{1u,2}(p > p_{int})$ will now vary according to the much larger v_{c+}.

We observe this general behaviour in our numerical analysis. Plotted in Fig. 3 are the dispersions of these two excitons for $K_{c+}^{-1} = 5$. We see that $E^{1u,1}(p)$ increases extremely rapidly for momenta up to $p \sim \Delta/2v_0$ but thereafter levels out, even decreasing. This increase is greater than would be predicted from the relativistic dispersion, $((\Delta^{1u,1})^2 + p^2 v_{c+}^2)^{1/2}$, suggesting that charge and spin, even at the smallest momenta, are intricately linked, leading to an even stronger renormalization of the effective mass. If however we combine the renormalization due to v_{c+} with the logarithmic correction $p^2 log(p)$, to the exciton self-energy, [12, 13] we can understand the observed behaviour. Complementarily, $E^{1u,2}(p)$ initially displays a weak momentum dependence but then increases with a velocity approximately $v_{c+}/2$ for $p > p_{int}$.

Finally we touch upon the excitonic signal in absorption spectra. This signal is proportional to the imaginary part of the current-current correlator. It is straightforward to compute the necessary matrix elements of the current operator within the framework of TCSA+NRG.[20] We find, as indicated in Fig. 1, that $\Delta^{1u,1}$ has by far the strongest signal. While $\Delta^{1u,2}$ should be visible in an absorption spectra, $\Delta^{1u,3}$, with a weighting 1/1000 of $\Delta^{1u,1}$ is effectively dark although could be detected indirectly through its effects on the temperature dependence of the excitonic radiative lifetime [13].

In conclusion, we have argued for, using a fully many-body, non-perturbative approach, new features in the excitonic spectrum of carbon nanotubes. We have shown that with a given subband, optically active excitons appear in *finite* hierarchies. We have also shown that the single particle sector experiences extremely strong renormalization so swapping the beginning of the particle-hole continuum with the two-exciton continuum. Further work will include studying the effects of backscattering interactions in the tubes (not treated here) together with intersubband interactions. More generally, we have demonstrated a robust method able to treat continuum representations of arbitrary one-dimensional systems.

RMK acknowledges support from the US DOE (DE-AC02-98 CH 10886) together with helpful discussions with V. Perebeinos, M. Sfeir, and A. Tsvelik.

[1] J. A. Misewich et al., Science **300**, 783 (2003).
[2] M. J. O'Connell et al., Science **297**, 593 (2002).
[3] J.-C. Charlier et al., Rev. Mod. Phys. **79**, 677 (2007).
[4] F. Wang et al., Science **308**, 838 (2005).
[5] O. N. Torrens et al., Phys. Rev. Lett. **101**, 157401 (2008).
[6] H. Lin et al., Nature Materials **9**, 235 (2010).
[7] T. Ogawa, T. Takaghara, Phys. Rev. B **44**, 8138 (1991).
[8] H. Ajiki and T. Ando, J. Phys. Soc. Jph. **62**, 1255 (1993); ibid. **65**, 505 (1996); C. Kane and E. Mele, Phys. Rev. Lett. **78**, 1932 (1997).
[9] L. Levitov, A. Tsvelik, Phys. Rev. Lett. **90**, 016401 (2003).
[10] M. Rohlfing, S. Louie, Phys. Rev. B **62**, 4927 (2000).
[11] V. Perebeinos et al., Phys. Rev. Lett. **92**, 257402 (2004).
[12] C. Kane, E. Mele, Phys. Rev. Lett. **93**, 197402 (2004).
[13] V. Perebeinos et al., Nano Lett. **5**, 2495 (2005).
[14] J. Maultzsch et al., Phys. Rev. B **72**, 241402 (2005); D. Kammerlander et al., Phys. Rev. Lett. **99**, 126806 (2007).
[15] J. Deslippe et al., Nano Lett. **9**, 1330 (2009).
[16] W. DeGottardi et al., Phys. Rev. B **79**, 205421 (2009).
[17] R. Egger and A. O. Gogolin, Eur. Phys. J. B **3**, 281 (1998).
[18] C. Kane et al., Phys. Rev. Lett. 79, 5086 (1997).
[19] V. P. Yurov and Al. B. Zamolodchikov, Int. J. Mod. Phys. A 6, 4557 (1991).
[20] R. M. Konik and Y. Adamov, Phys. Rev. Lett. **98**, 147205 (2007).
[21] R. M. Konik, see accompanying supplementary material.
[22] S. Lukyanov and A. Zamolodchikov, Nucl. Phys. B. **493**, 571 (1997).
[23] Al. Zamolodchikov, J. Mod. Phys. A **10**, 1125 (1995).